Title

Identification of C2CD4A as a human diabetes susceptibility gene with a role in β cell insulin secretion

Journal

Proceedings of the National Academy of Sciences of the United States of America, 116(40)

ISSN

0027-8424

Authors

Kuo, Taiyi
Kraakman, Michael J
Damle, Manashree
et al.

Publication Date

2019-10-01

DOI

10.1073/pnas.1904311116

Peer reviewed

Identification of *C2CD4A* as a human diabetes susceptibility gene with a role in β cell insulin secretion

Taiyi Kuo[a], Michael J. Kraakman[a], Manashree Damle[b,c], Richard Gill[a], Mitchell A. Lazar[b,c,1], and Domenico Accili[a,1]

[a]Department of Medicine, Berrie Diabetes Center, Columbia University College of Physicians and Surgeons, New York, NY 10032; [b]The Institute for Diabetes, Obesity, and Metabolism, University of Pennsylvania Perelman School of Medicine, Philadelphia, PA 19104; and [c]Division of Endocrinology, Diabetes, and Metabolism, Department of Medicine, University of Pennsylvania Perelman School of Medicine, Philadelphia, PA 19104

Contributed by Mitchell A. Lazar, July 31, 2019 (sent for review March 14, 2019; reviewed by Alvin C. Powers and Andrew F. Stewart)

Fine mapping and validation of genes causing β cell failure from susceptibility loci identified in type 2 diabetes genome-wide association studies (GWAS) poses a significant challenge. The *VPS13C-C2CD4A-C2CD4B* locus on chromosome 15 confers diabetes susceptibility in every ethnic group studied to date. However, the causative gene is unknown. FoxO1 is involved in the pathogenesis of β cell dysfunction, but its link to human diabetes GWAS has not been explored. Here we generated a genome-wide map of FoxO1 superenhancers in chemically identified β cells using 2-photon live-cell imaging to monitor FoxO1 localization. When parsed against human superenhancers and GWAS-derived diabetes susceptibility alleles, this map revealed a conserved superenhancer in *C2CD4A*, a gene encoding a β cell/stomach-enriched nuclear protein of unknown function. Genetic ablation of C2cd4a in β cells of mice phenocopied the metabolic abnormalities of human carriers of *C2CD4A*-linked polymorphisms, resulting in impaired insulin secretion during glucose tolerance tests as well as hyperglycemic clamps. C2CD4A regulates glycolytic genes, and notably represses key β cell "disallowed" genes, such as *lactate dehydrogenase A*. We propose that *C2CD4A* is a transcriptional coregulator of the glycolytic pathway whose dysfunction accounts for the diabetes susceptibility associated with the chromosome 15 GWAS locus.

C2cd4a | FoxO1 | diabetes | epigenetics | GWAS

Type 2 diabetes (T2D) affects an estimated 30 million people in the United States alone, including ∼7 million who are unaware of having the disease, while 700,000 more are expected to be diagnosed every year (1). The disease is caused by insulin resistance in peripheral tissues and pancreatic β cell failure. Insulin resistance precedes β cell failure, and the β cell's inability to compensate for the increased demand of insulin production results in hyperglycemia. Thus, β cell dysfunction is pivotal in the pathogenesis of T2D (2).

Genome-wide association studies (GWAS) across different ethnicities and whole-genome sequencing have identified SNPs associated with increased risk of T2D spread across 90 loci meeting statistical significance at the whole-genome level (3–5). However, in only a small fraction of these loci has a causative gene emerged (6–8). Thus, fine-mapping and identification of causative genes remain a research challenge.

A restricted network of transcription factors directs β cell maintenance and function, influences chromatin architecture and gene expression, and arguably underlies the genetic predisposition to T2D (9–11). They do so through transcriptional hubs or superenhancers (12, 13). The mechanistic link between T2D GWAS loci, β cell maintenance transcription factors, and superenhancers is elusive. A glaring gap in knowledge in this area relates to FoxO1, a key factor involved in the pathogenesis of islet β cell dysfunction in rodents and humans (14–16), whose role in diabetes-associated superenhancers and human GWAS loci has not been investigated (12, 17). This gap in knowledge can be attributed to the difficulty of monitoring the localization of endogenous FoxO1 in vivo which, combined with the low efficiency of antibodies to immunoprecipitate FoxO1, have hampered efforts to catalog its genomic targets. To circumvent this obstacle, we generated FoxO1-GFP^{Venus} (Venus) reporter knockin mice, and utilized 2-photon microscopy to track its subcellular localization in pancreatic β cells. We next performed genome-wide FoxO1 chromatin immunoprecipitation sequencing (ChIP-seq) to identify its genomic targets as well as superenhancers encompassing FoxO1 sites. A comparative analysis of human islet and murine β cell superenhancers revealed *C2CD4A*, a gene encoding an IL-1β–induced nuclear protein (18) embedded among several SNPs conferring susceptibility to human T2D (19–21). β Cell–specific ablation of C2cd4a in mice causes glucose intolerance due to reduced insulin secretion, and impairs glucose-induced insulin release in vivo as well as ex vivo. Although the molecular function of C2cd4a has yet to be defined, gain-of-function experiments indicate that it regulates the glycolytic cascade at the transcriptional level, acting possibly as a FoxO1 coregulator. These findings integrate mechanistic evidence in experimental animals with human genetics to illustrate a potential new pathway of β cell failure.

Results

Determination of Conditions to Elicit Nuclear FoxO1. Analyses of FoxO1 DNA binding sites have been hampered by a dearth of suitable antibodies, and by the low expression levels of this

Significance

Many human genomic loci have been linked to diabetes, but the actual dysregulated gene is often unclear. The *VPS13C-C2CD4A-C2CD4B* locus on human chromosome 15 is linked to reduced function of insulin-producing β cells in diabetes by integrating human genetic loci with super-enhancers bound by transcription factor FoxO1. Epigenomic studies pinpoint C2CD4A as the critical FoxO1 target gene in this locus. Mice lacking C2cd4a in β cells recapitulate the β cell dysfunction seen in human carriers of the susceptibility allele at this locus. C2cd4a localizes to the nucleus and regulates genes involved in insulin secretion. As a regulator of insulin secretion, C2cd4a may be an attractive new target for diabetes therapies.

Author contributions: T.K., M.A.L., and D.A. designed research; T.K. and M.J.K. performed research; T.K., M.J.K., M.D., R.G., M.A.L., and D.A. analyzed data; and T.K., M.D., R.G., M.A.L., and D.A. wrote the paper.

Reviewers: A.C.P., Vanderbilt University; and A.F.S., Mount Sinai Hospital.

Conflict of interest statement: M.A.L. is an Advisory Board Member for Pfizer, Inc. and Eli Lilly and Co., and a consultant to Novartis. He has received research funding from Merck, Inc. and Pfizer, Inc. for studies other than the present work. D.A. is cofounder and director of Forkhead Biotherapeutics, Corp., and an Advisory Board Member to Eli Lilly and Co.

Data deposition: The data reported in this paper have been deposited in the Gene Expression Omnibus (GEO) database, https://www.ncbi.nlm.nih.gov/geo (accession nos. GSE131947 and GSE132200).

[1]To whom correspondence may be addressed. Email: lazar@pennmedicine.upenn.edu or da230@cumc.columbia.edu.

This article contains supporting information online at www.pnas.org/lookup/suppl/doi:10.1073/pnas.1904311116/-/DCSupplemental.

First published September 16, 2019.

transcription factor. These issues are especially challenging in pancreatic β cells, because FoxO1 is predominantly cytoplasmic in the resting state, due to constitutive Akt-dependent phosphorylation (*SI Appendix*, Fig. S1) (22). To circumvent these issues and interrogate the genomic FoxO1 binding sites, we used BAC-mediated homologous recombination in embryonic stem cells to generate a knockin allele in mice encoding a GFP variant, Venus, fused to the COOH terminus of endogenous FoxO1. When bred to homozygosity, these mice only express the FoxO1–Venus fusion protein (Fig. 1 *A*–*I*).

Using this tool, we evaluated FoxO1 nuclear translocation in β cells using 2-photon microscopy, in order to maximize our ability to perform informative ChIP experiments (*SI Appendix*, Fig. S2*A*). Varying the glucose concentration in the medium, in the absence of serum to remove growth factors that promote FoxO1 nuclear exclusion, was only partly effective in increasing the percentage of cells with nuclear FoxO1 from 19 to 34% (*SI Appendix*, Fig. S2 *B*–*D*). This level of enrichment was insufficient to perform chromatin isolation. In contrast, treatment with the nuclear export inhibitor, leptomycin B, resulted in nuclear accumulation of FoxO1 within an hour (Movie S1). By 2 h, FoxO1 immunofluorescence was nearly exclusively nuclear (*SI Appendix*, Fig. S2 *E* and *F*). These results provide a framework to interrogate FoxO1 target genes.

A Network of Genome-Wide FoxO1 Targets Underpinning Its Role in β Cells. We performed ChIP-seq in leptomycin B-treated islets pooled from 16 Venus mice per ChIP-seq experiment. The sequencing tags were aligned to the mouse genome (mm10). Only the unique alignments without duplicate reads were normalized to input DNA for peak calling by model-based analysis for ChIP-seq (MACS 1.4.2). Based on a stringent threshold (*P* value cutoff of 10^{-7} and 3% false-discovery rate [FDR]) (Fig. 1*J* and Dataset S1), HOMER de novo motif analysis with total filtered peaks established the optimal FoxO1 binding site as TGTTTAC with a *P* value of 10^{-292} (Fig. 1*K*). Twenty-five percent of FoxO1 binding sites mapped to proximal promoters (within 1 kb of the transcription start site, TSS), 4% to distal promoters (1 to 3 kb of TSS), 27% to introns, and 16% to distal intergenic regions (Fig. 1*L*). We found FoxO1 binding sites in the promoters of 6 of the 7 most common MODY genes: *Gck* (MODY2), *Hnf1α* (MODY3), *Pdx1* (MODY4), *Hnf1β* (MODY5), *NeuroD1* (MODY6), and *Klf11* (MODY7) (*SI Appendix*, Fig. S3 *A*–*F*), as well as in promoters of genes regulating β cell differentiation (*Nkx6-1*, *Isl1*, *MafA*, *FoxA1*, and *FoxA2*) (*SI Appendix*, Fig. S3 *G*–*K*), and maintenance (*Nkx2-2*, *Pax6*, and *Ldb1*) (*SI Appendix*, Fig. S3 *L*–*N*). These data are consistent with the important role of this transcription factor in β cell function. Using FIMO (23), we detected the FoxO1 consensus motif in nearly half of the above-mentioned genes: *FoxO1*, *FoxO3*, *Pax6*, *Gck*, *Hnf1α*, *Pdx1*, *NeuroD1*, and *FoxA2* (*SI Appendix*, Fig. S3 and Dataset S2). The identification of FoxO1 binding sites in the *FoxO1*, *-3a*, and *-6* promoters suggests that FoxO1 regulates its own expression and that of other members of this gene family (*SI Appendix*, Fig. S3 *O*–*Q*). There are no other sites for β cell master regulators in the *Foxo1* gene, providing a mechanism for the FoxO1 autoregulatory loop that leads to β cell dedifferentiation when FoxO1 degradation increases (24, 25).

Functional Validation of ChIP-Seq Data. To establish a functional correlation between FoxO1 DNA binding and gene regulation, we compared genes identified as FoxO1 targets by ChIP-seq with genes differentially expressed in FoxO1 knockout vs. WT β cells by RNA sequencing (26). We found 559 genes whose expression was altered in FoxO1 knockout β cells and encompassed FoxO1 binding sites (Dataset S3). Ingenuity pathway analysis identified RICTOR/protein translation, glucose metabolism, retinoid signaling, and mitochondrial oxidative phosphorylation as the top FoxO1-regulated pathways (*SI Appendix*, Table S1). In addition, manual curation of the data demonstrated a clustered enrichment of FoxO1 binding sites in several functionally related gene families,

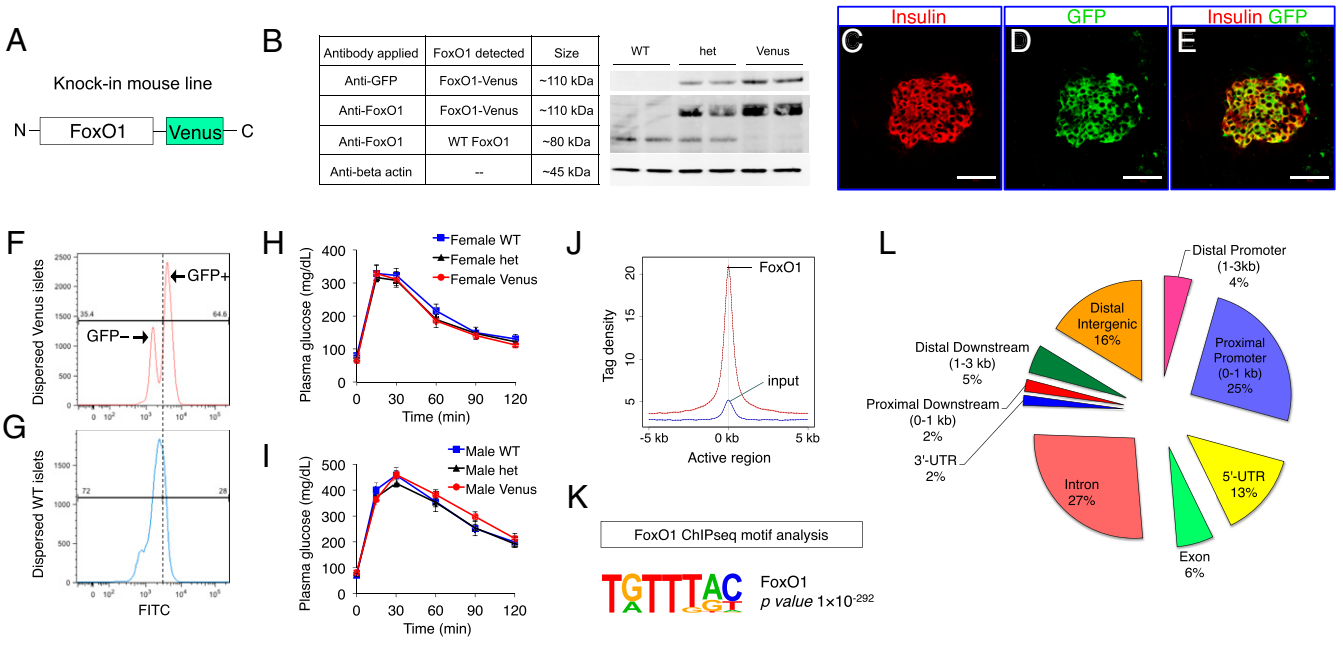

Fig. 1. FoxO1 ChIP-seq in Venus mice. (*A*) Knockin construct used to generate Venus mice. (*B*) Western blotting of pancreatic islets harvested from Venus mice. (*C*–*E*) Immunofluorescence staining with insulin and GFP antibody in the islet. (Scale bars, 50 μm.) (*F*–*G*) Flow cytometry analysis of dispersed (*F*) Venus and (*G*) WT islet cells. (*H* and *I*) Glucose tolerance tests of WT, heterozygous (het), and homozygous Venus (*H*) female (WT $n = 7$, het $n = 11$, Venus $n = 7$) and (*I*) male mice (WT $n = 5$, het $n = 15$, Venus $n = 8$). Data represent means ± SEM. (*J*) Average plot for FoxO1 ChIP-seq and input, where the *y* axis represents tag density across all active regions, shown in *x* axis. Tag density represents DNA fragment per 32-bp bin. (*K*) FoxO1 consensus motif generated by HOMER. (*L*) Pie chart showing the genomic distribution of FoxO1 binding sites.

including insulin/IGF signaling, vesicle trafficking, K^+ and Ca^{2+} channels, hormone processing, and stress response (Dataset S4). These data indicate that the primary biological functions of FoxO1 can be imputed to direct regulation of DNA transcription.

FoxO1 is activated in response to insulin resistance (*SI Appendix*, Fig. S1 *A*–*C*). However, the extent to which this activation results in increased enhancer occupancy by FoxO1 is unknown. In other words, FoxO1 could be nuclear, but inactive. To establish the functional relevance of the FoxO1 enhancer binding sites, we interrogated enhancer distribution at active chromatin sites using genome-wide ChIP with an antibody against acetylated histone 3 lysine 27 (H3K27ac) in *db*/*db* mice (Dataset S5 and Dataset S6). To this end, we introduced a ROSA-Tomato allele into *db*/*db* mice, then sorted β cells and subjected them to ChIP-seq with the above-mentioned antibody. We found increased levels of H3K27ac genome-wide in *db*/*db* β cells (Fig. 2 *A* and *B*).

Next, we sorted H3K27ac regions associated with promoters (defined as ±3 kb from the TSS) or distal enhancers, and mined transcription factor binding motifs in distal enhancers characterized by increased or decreased H3K27ac marks in *db*/*db* (Fig. 2*C*). Motifs of activated transcription factor binding should be enriched in hyperacetylated enhancers, whereas motifs of suppressed transcription factors should be enriched in hypoacetylated enhancers. Indeed, FoxO1 was the top motif found within activated enhancers in *db*/*db* β cells (Fig. 2*D*), consistent with the ChIP-seq and functional data in mice fed a high-fat diet (*SI Appendix*, Fig. S1 *A*–*C*). Other activated motifs included 2 important β cell transcription factors, NFAT and FoxA2 (Fig. 2*D*) (27–29).

Conversely, the top motifs within hypoacetylated enhancers were Hmbox1 and Gli (Fig. 2*E*). The role of Hmbox1 (30) in β cells is unknown, whereas Gli mediates hedgehog signaling, a regulator of insulin secretion (31) and β cell dedifferentiation (32). These observations provide evidence of activated FoxO1 at the enhancers in β cells in response to insulin-resistant diabetes (25, 33), critically validating the ChIP-seq data.

Enrichment of FoxO1 Superenhancers. Superenhancers mark genes underpinning β cell identity (12, 13). Using H3K27ac ChIP-seq in FAC-sorted β cells, we identified 1,054 superenhancers and mapped FoxO1 sites to these regions. Strikingly, ∼89% of β cell superenhancers (935 of 1,054) encompassed FoxO1 peaks, and accounted for ∼22% of FoxO1 binding sites (Dataset S7). As a comparison, superenhancers account for ∼13% of Pdx1, ∼24% of NeuroD1, ∼14% of MafA, and ∼12% of FoxA2 sites (17, 34) (Dataset S7). Superenhancers are thought of as hubs of functionally related transcription factors; thus, we incorporated key β cell factors Pdx1, MafA, NeuroD1, and FoxA2 into our analysis (17, 34). We found Pdx1 peaks in 82% of β cell superenhancers, NeuroD1 peaks in 47%, MafA peaks in 35%, and FoxA2 peaks in 46%. Furthermore, we identified a subset of 74 FoxO1-exclusive superenhancers, corresponding to 7% of all superenhancers (Dataset S8). This list included master regulators of β cell differentiation, *Hes1*; mitochondrial biogenesis, *Nfe2l2*; and β cell development, *Hnf1β* and *FoxA2*. When we ranked the 1,054 superenhancers based on transcription factor enrichment, the top 10% included a virtual "who's who" of β cell genes: *Iapp*, *MafA*, *Pax6*, *NeuroD1*, *Pdx1*, *Dnmt3*, *Pcsk2*, *Glut2*, *Vamp2*, *Kcnj11*, *Txnip*, and *Chga* (Dataset S7).

Conservation of Human and Murine Superenhancers. Using the liftOver function of the University of California, Santa Cruz genome browser (35), we converted newly annotated human islet class I active enhancers (hg19) with high occupancy of H3K27ac and Mediator (12, 36), to mouse coordinates (mm10). The goal was to investigate whether mouse β cell superenhancers are conserved and functional in humans. We found 601 (57%) mouse superenhancers

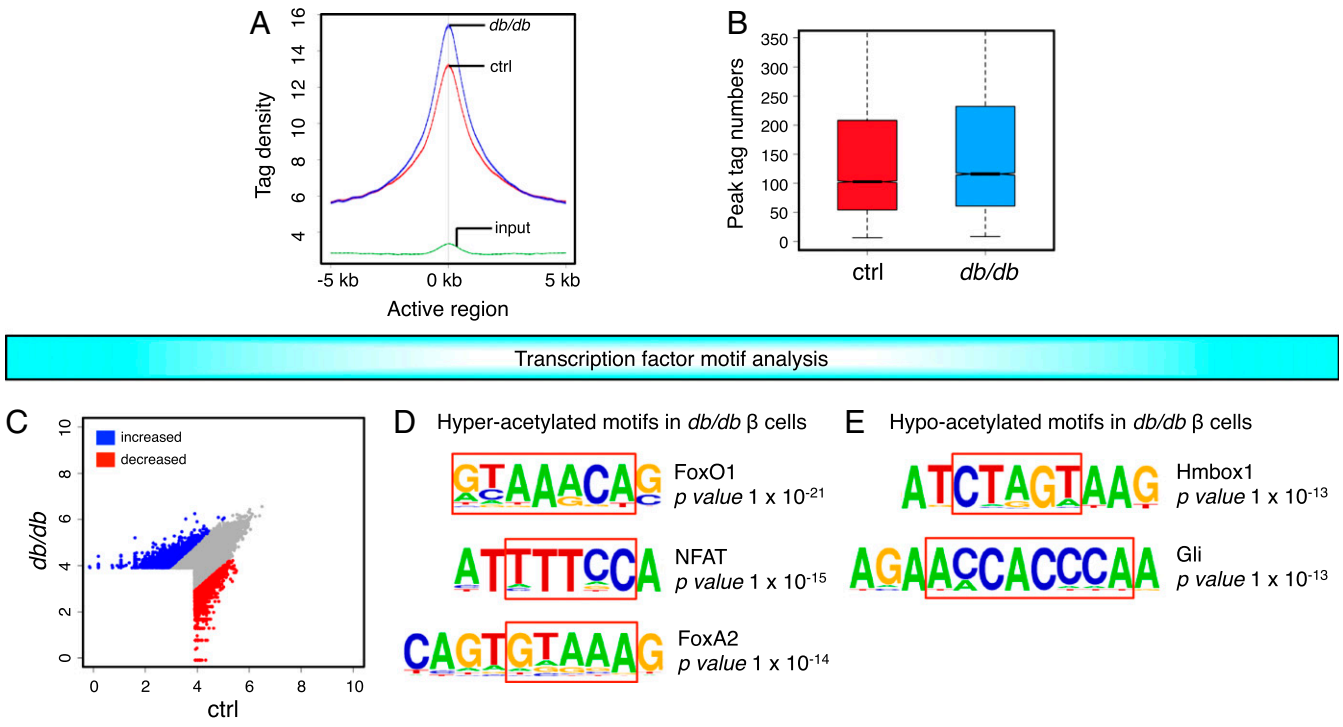

Fig. 2. H3K27ac enhancer analysis in *db*/*db* β cells identified FoxO1. (*A*) Average plot for H3K27ac ChIP-seq, where *y* axis represents tag density across all active regions, shown in the *x* axis. (*B*) Number of tags in the active peak regions in WT and *db*/*db* β cells. (*C*–*E*) Transcription factor motif analysis in distal enhancer regions. (*C*) The parameters for differential peak calling are the following: Fragments per kilobase of DNA per 10 million mapped reads (FPKTM) > 30 for at least 1 of the groups, and fold-change (FC) > 1.5. (*D*) List of hyperacetylated motifs. (*E*) Hypoacetylated motifs. For each transcription factor motif, consensus or partial consensus sequence is boxed, and *P* value is shown.

shared with human enhancers (Fig. 3*A* and Dataset S9), including *C2cd4a/b*, *Cyb5r3*, *Dnmt3a*, *FoxA2*, *Gck*, *Gipr*, *Glp1r*, *Hes1*, *Hnf1α*, *Hnf1β*, *Ins2*, *Isl1*, *MafA*, *NeuroD1*, *Nfatc2*, *Pax6*, *Pdx1*, *Slc2a2*, and *Slc30A8*. Of these, 17 superenhancers are FoxO1-exclusive, including *Hnf1β* and *FoxA2* (Dataset S10).

We queried the 90 consensus loci identified in human type 2 diabetes GWAS (6, 37), and identified FoxO1 sites in 42% of their promoters (38 of 90). Of these, 34% (13 of 38) are within β cell superenhancers (*Wfs1*, *Hnf1β*, *Slc30A8*, *Srr*, *Prc1*, *Gck*, *Ap3s2*, *Zmiz1*, *Glis3*, *Bcar1*, *Grk5*, *Mphosph9*, and *Hnf1α*) (*SI Appendix*, Fig. S4), consistent with a role in β cells. Among them, *Wfs1* (38), *Hnf1β*, *Slc30A8*, *Gck*, and *Hnf1α* are essential β cell genes. As a comparison, we extended the analysis to include Pdx1, MafA, NeuroD1, and FoxA2. Twenty-five percent of GWAS susceptibility alleles localize to murine β cell superenhancers (23 of 90). Among these, Pdx1 was found in 20 of the 23, FoxO1 in 19, NeuroD1 in 16, FoxA2 in 13, and MafA in 11 (*SI Appendix*, Fig. S5). Thus, similar to human islet superenhancers (12), mouse β cell superenhancers serve as transcriptional hubs.

Superenhancer at *C2cd4b-C2cd4a-Vps13c*. We focused on a FoxO1 superenhancer shared between human and mouse β cells that encompassed the *C2cd4b-C2cd4a-Vps13c* locus. It included 32 sites shared among 5 transcription factors (FoxO1, Pdx1, MafA, FoxA2, NeuroD1) (Fig. 3*B* and Dataset S11). Several SNPs at the *VPS13C-C2CD4A-C2CD4B* locus have been associated with type 2 diabetes in GWAS from virtually every ethnic group studied to date (19, 39, 40). The mouse locus encoding *C2cd4b-C2cd4a-Vps13c* is syntenic with human chromosome 15, although the genes are in reverse order. Of the 3 genes encoded at this locus, 2 (*VPS13C* and *C2CD4A*) show an association between mRNA expression and a risk allele (rs7163757) based on expression quantitative trait loci (eQTL) (21). However, *Vps13c* ablation in mice does not affect β cell function (21). Interestingly, in separate studies of histone modifications in dedifferentiating β cells, we detected reduced activation marks (histone H3 lysine 4 trimethylation) (Fig. 3*C*) (26) and decreased expression of *C2cd4a* in FoxO1-deficient β cells (Fig. 3*D*) (26).

To confirm FoxO1 binding to the *C2cd4b-C2cd4a* locus, we performed ChIP-qPCR, and validated all sites between *C2cd4b* and *C2cd4a* (Fig. 3*E*). We also found sites in the *C2cd4b*, *C2cd4a*, and *Vps13c* promoter; however, expression of *C2cd4b* or *Vps13c* was not altered in the absence of FoxO1, suggesting that they are not FoxO1 targets in β cells. To test if the *C2cd4b-C2cd4a-Vps13c* superenhancer marks cell-type–specific genes, we performed gene-expression analysis in an array of metabolic tissues. Among the 14 tissues surveyed, we found that C2cd4a is highly expressed only in islets and stomach from mice of both genders (Fig. 3 *F* and *G*). These data raised the possibility that *C2cd4a* encodes the diabetes susceptibility gene identified at this

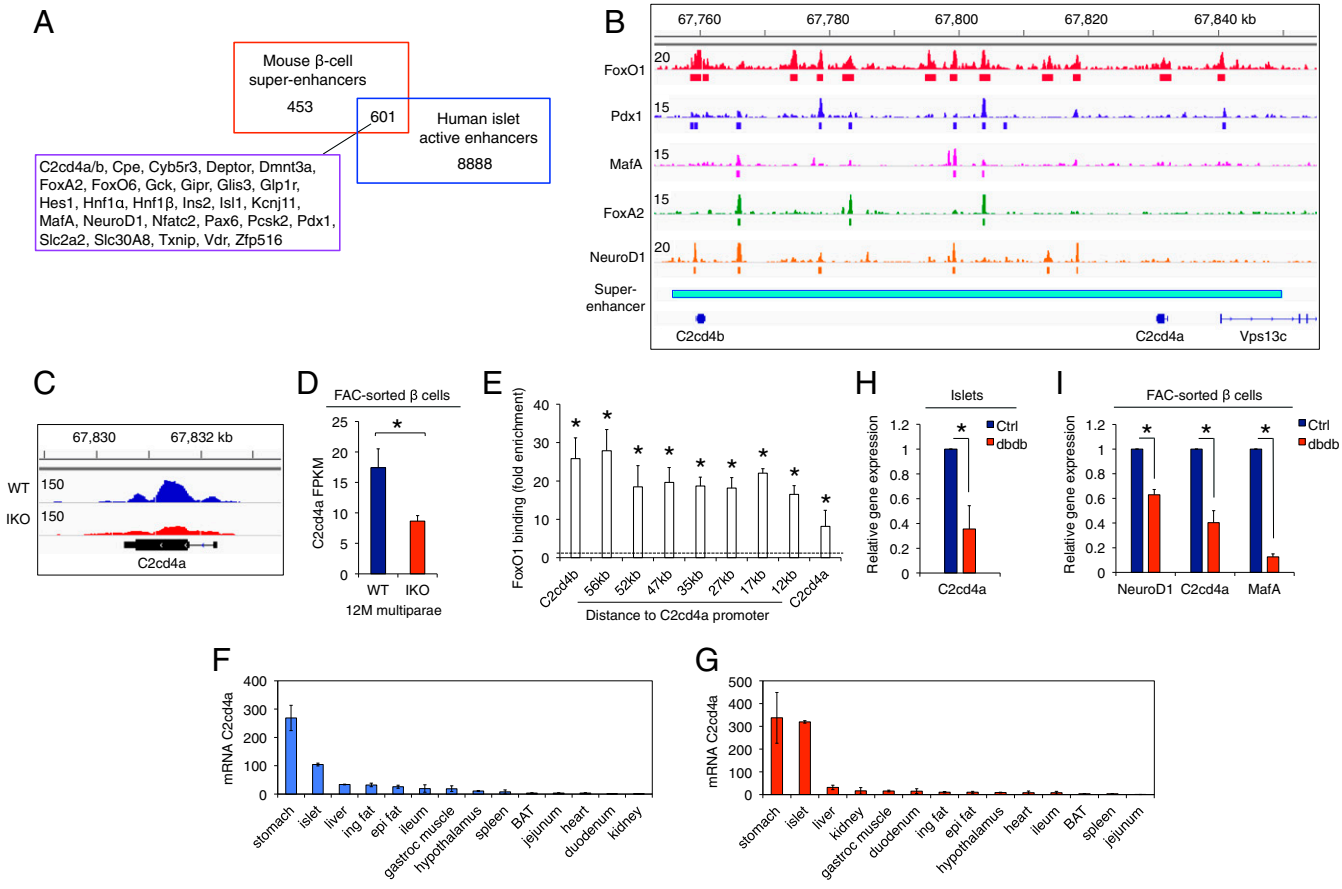

Fig. 3. FoxO1 superenhancer at the diabetes susceptibility gene C2cd4a. (*A*) Comparison of mouse β cell superenhancers and human islet active enhancers. (*B*) Integrative genomic viewer shows FoxO1, Pdx1, MafA, FoxA2, and NeuroD1 binding, and superenhancer at the *C2cd4b-C2cd4a-Vps13c* locus. (*C*) ChIP-seq of trimethylated H3K4me3 ($n = 3$) in FACS-sorted β cells from 12-mo-old multiparous WT and β cell–specific FoxO1 knockouts (IKO). C2cd4a region is shown. (*D*) RNA profile of C2cd4a in FAC-sorted β cells from 12-mo-old multiparous WT and IKO ($n = 3$). (*E*) ChIP-qPCR validation for FoxO1 binding sites (shown in *B*) between C2cd4b and C2cd4a, as well as in C2cd4b and C2cd4a promoter ($n = 3$). (*F* and *G*) Gene-expression analysis of C2cd4a in a panel of metabolic tissues from (*F*) male and (*G*) female WT mice ($n = 3$ for each group). (*H* and *I*) C2cd4a expression analysis from (*H*) purified islets and (*I*) FACS-sorted β cells in control and *db/db* mice ($n \geq 3$ for each group). Data represent means ± SEM, $^*P < 0.05$ by Student's *t* test.

locus. Furthermore, we surveyed *C2cd4a* expression in *db*/*db* mice, and found it to be decreased in islets and FACS-sorted β cells, along with *NeuroD1* and *MafA* (Fig. 3 *H* and *I*).

Functional Studies of C2cd4a. To investigate C2cd4a function in vivo, we generated β cell–specific *C2cd4a* knockout mice (CKO) using *insulin-Cre* transgenics to drive somatic recombination (Fig. 4*A*). We purified islets from WT and CKO mice, and showed an ∼95% decrease of *C2cd4a* mRNA in the latter (Fig. 4*B*). We obtained a similar decrease when we FACS-sorted β cells from CKO islets (Fig. 4*C*), indicating that C2cd4a is enriched in β cells.

We performed glucose tolerance tests and found that 12-wk-old CKO mice on a normal diet are glucose intolerant (Fig. 4 *D* and *E*) and display reduced insulin levels in the fed state (Fig. 4*F*), without changes in body weight. This phenotype recapitulates the elevated glucose and lower plasma insulin levels after an oral glucose tolerance test in humans with *C2CD4A*-associated SNPs (20, 40). We also tested glucose-stimulated insulin secretion ex vivo in purified islets. Indeed, CKO islets showed a ∼50% reduction of the response to glucose compared to WT (Fig. 4*G*).

To assess insulin secretory capacity in vivo, we performed hyperglycemic clamps. We infused glucose intravenously to raise glycemia to ∼300 mg/dL (Fig. 4 *H* and *I*), and measured the rate of glucose infusion necessary to maintain this level of hyperglycemia. Consistent with the glucose tolerance test, CKO showed an ∼30% reduction in glucose infusion rates compared to WT (Fig. 4 *J* and *K*). This was due to an ∼35% decrease in insulin secretory capacity (Fig. 4 *L* and *M*). Overall, these data establish an important role of C2cd4a in insulin secretion.

C2cd4a Regulates the Glycolytic Gene Network. C2cd4a bears no sequence resemblance to other known proteins. To begin to understand its mechanism of action, we performed loss- and gain-of-function experiments in MIN6 cells. Consistent with previous reports (18, 41), we found an induction of *C2cd4a* in IL-1β–treated islets and MIN6 cells (Fig. 5 *A* and *B*). Using adenovirus-mediated transduction of MIN6 cells and primary islets, we confirmed that C2cd4a localizes to the nucleus (Fig. 5 *C*–*H*) (18).

We inactivated C2cd4a in MIN6 cells using CRISPR/Cas9-mediated loss-of-function. After nucleofection, we fluorescently selected GFP-tagged clones of control (Fig. 5*I*) and mCherry-tagged C2cd4a knockout cells (Fig. 5*J*), and cultured them as polyclonal populations to avoid clonal artifacts in functional assays. Expression analysis demonstrated successful ablation of C2cd4a (Fig. 5*K*). Consistent with the mouse data, we found that C2cd4a ablation significantly compromised glucose- and arginine-stimulated insulin secretion (Fig. 5*L*).

To investigate the mechanism of C2cd4a-regulated insulin secretion, we performed RNA sequencing in MIN6 cells overexpressing C2cd4a (Dataset S12). Ingenuity pathway analysis identified glycolysis (*z* score –3.051), AMPK signaling (*z* score –2.117), and PKA signaling (*z* score 1.524) as key C2cd4a target networks (*SI Appendix*, Table S2). Several features of the gene profile of C2cd4a gain-of-function stood out. C2cd4a represses Gc (vitamin D-binding protein), an α-cell–restricted gene that is induced in dedifferentiated β cells and contributes to β cell dysfunction in the face of metabolic challenge (26).

β-Cells take up glucose via Glut2, phosphorylate it using the low K_m glucokinase, and perform strictly aerobic glycolysis to couple glucose metabolism with insulin secretion. Thus, in addition to genes

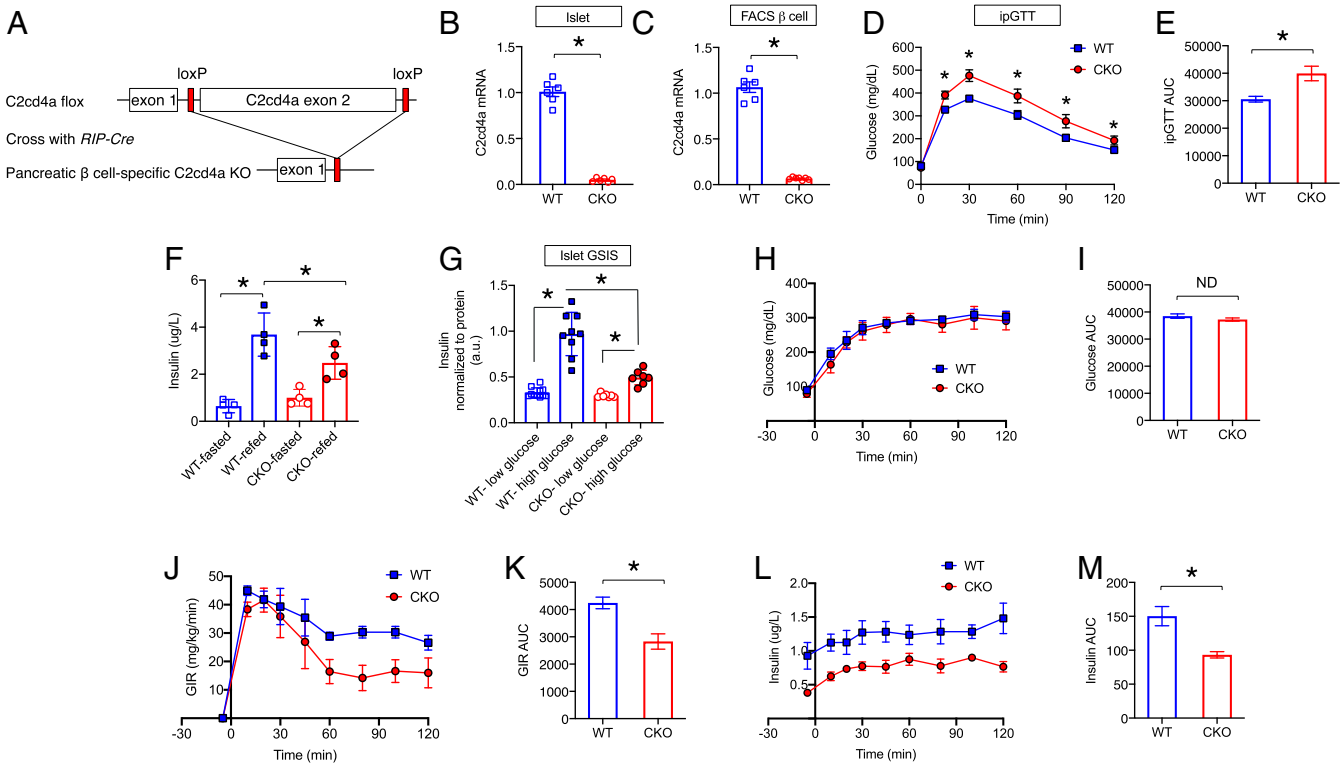

Fig. 4. Functional studies of β cell–specific CKO mice. (*A*) Generation of CKO mice. (*B* and *C*) C2cd4a expression in *B* islets ($n = 3$ for each genotype) and (*C*) FACS-sorted β cells ($n = 3$ for each genotype). (*D*) Intraperitoneal glucose tolerance tests in 3-mo-old WT ($n = 4$) and CKO ($n = 3$) mice. (*E*) Area under the curve for glucose tolerance tests in *D*. (*F*) Insulin secretion in 16-h fasted or 2-h refed WT ($n = 4$) and CKO ($n = 4$) mice. (*G*) Ex vivo glucose-stimulated insulin secretion in purified islets from 4-mo-old WT ($n = 7$) and CKO ($n = 7$). (*H* and *I*) Glucose levels and area under the curve (AUC) (*I*) during hyperglycemic clamps. (*J* and *K*) Glucose infusion rates and AUC (*K*) during hyperglycemic clamps. (*L and M*) Plasma insulin levels and AUC (*M*) during hyperglycemic clamps. $n = 4$ mice per genotype. Data represent means ± SEM, $^*P < 0.05$ by Student's *t* test.

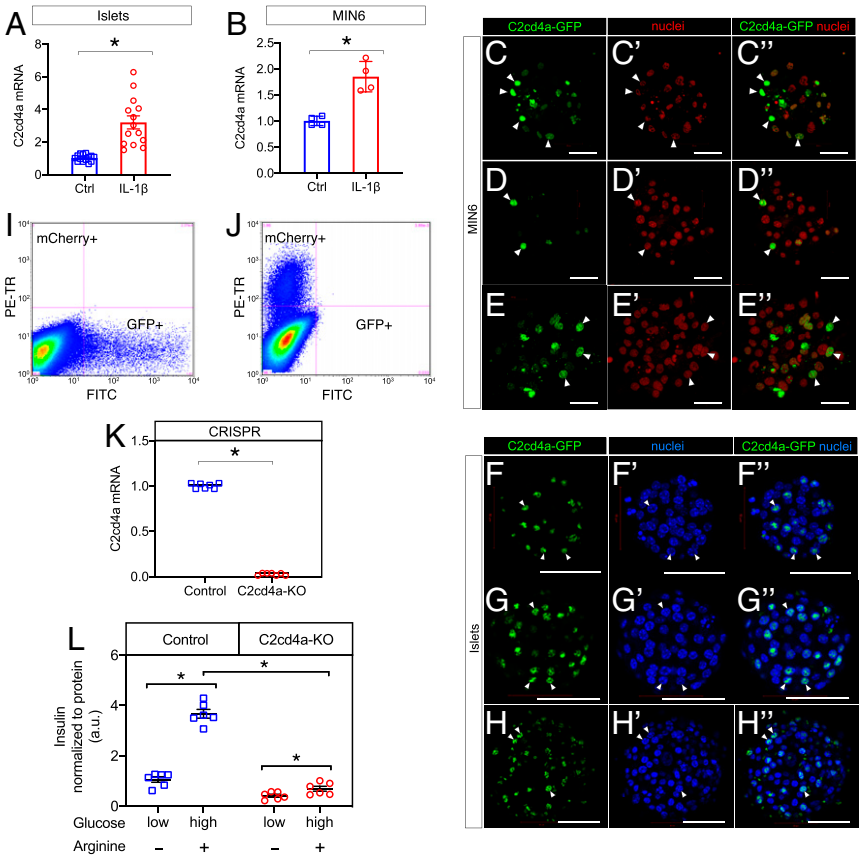

Fig. 5. C2cd4a, an IL-1β–induced nuclear protein, regulates insulin secretion. (*A* and *B*) Induced C2cd4a gene expression in response to IL-1β in *A* islets and (*B*) MIN6 cells ($n \geq 3$ for each group). (*C–H*) Cellular localization of C2cd4a protein in *C–E* MIN6 cells and (*F–H*) primary mouse islets. Nuclei are shown in red in *C–E* and blue in *F–H*, while C2cd4a-GFP are shown in green. Arrowhead indicates colocalization. (Scale bars, 50 μm.) $n = 3$ for each group. (*I* and *J*) Flow cytometric plots pregated on MIN6 cells electroporated with (*I*) control GFP or (*J*) mCherry-tagged C2cd4a CRISPR construct. FITC (*x* axis) indicates the levels of GFP fluorescence, and PE-TR (*y* axis) shows the levels of mCherry fluorescence. (*K*) C2cd4a expression in GFP control and *C2cd4a* knockout MIN6 cells ($n = 7$). (*L*) Glucose and arginine-stimulated insulin secretion in GFP control and *C2cd4a* knockout MIN6 cells ($n = 6$ for each group). Data represent means ±SEM, $^*P < 0.05$ by Student's *t* test.

involved in the glycolytic pathway, they maintain a list of so-called "disallowed" genes that prevent anaerobic glycolysis. The most notable example of disallowed genes is *lactate dehydrogenase A* (*Ldha*), repression of which is required to avoid lactic acid-dependent insulin release, and to maintain coupling of pyruvate through oxidative phosphorylation (42, 43). This gene was potently inhibited by C2cd4a (P value 6×10^{-100}), as were Glut2, glucokinase, and 8 of the 10 genes involved in enzymatic steps of glycolysis, including glucose-6-phosphate isomerase (*Gpi*, step 2 of glycolysis), phosphofructokinase (*Pfk*, step 3), aldolase (*Aldo*, step 4), triosephosphate isomerase (*Tpi1*, step 5), phosphoglycerate kinase (*Pgk1*, step 7), phosphoglycerate mutase (*Pgam1*, step 8), enolase (*Eno1*, step 9), and pyruvate kinase (*Pkm*, step 10) (Fig. 6*A*). In addition, fructose bis-phosphatase was induced, which is predicted to further inhibit glycolysis. Interestingly, a subset of enzymes in fatty acid oxidation were increased, while pyruvate dehydrogenase kinase was decreased, removing a constraint on mitochondrial fatty acid oxidation (Fig. 6*A*).

This gene-expression pattern bore an uncanny resemblance to that associated with FoxO1 gain-of-function, where overexpression of FoxO1 inhibits glucose utilization and primes the β cell for fatty acid oxidation (44), consistent with the notion that C2cd4a is a FoxO1 target. C2cd4a lacks a DNA binding domain, but 26 of its top 100 upstream regulators are transcription factors, suggesting that it functions as a transcriptional coregulator (Fig. 6*B*). Indeed, 8 of the 10 glycolytic genes regulated by C2cd4a also possess FoxO1 binding sites (Fig. 6 *C–L*). These data suggest that C2cd4a acts as a master-regulator of glycolytic genes, possibly in cooperation with FoxO1 (Fig. 7 *A* and *B*). Its suppression of disallowed genes is striking (Fig. 7*C*), as it's consistent with a homeostatic role in β cell function.

Discussion

The main findings of this work are: 1) integrated analyses of human GWAS-associated superenhancers and FoxO1-associated mouse superenhancers identify *C2CD4A*, within a human diabetes susceptibility locus on chromosome 15, as having an important role in insulin secretion; 2) functional analyses of C2cd4a in knockout mice and insulinoma cells are consistent with an important role of this protein in insulin secretion, possibly as a master regulator of glycolysis and an enforcer of β cell "disallowed" genes; 3) FoxO1 occupies ∼90% of β cell superenhancers, including those regulating MODY genes, and key β cell transcription factors and signaling pathways, such as insulin/IGF, mammalian target of rapamycin (mTOR)/RICTOR, glucose metabolism, mitochondrial function, and vesicle trafficking; these enhancers become enriched in insulin-resistant *db*/*db* mice, consistent with a role of this network in the response to islet stress.

We identified the *C2cd4b-C2cd4a-Vps13c* locus through integrated analyses of FoxO1, Pdx1, MafA, NeuroD1, and FoxA2 ChIP-seq, as well as comparisons of human and murine superenhancers. Various SNPs in the *VPS13C-C2CD4A-C2CD4B* superenhancer (12, 13, 45) have been linked to T2D in GWAS (19, 39, 40, 46). We summarized the associations of different risk

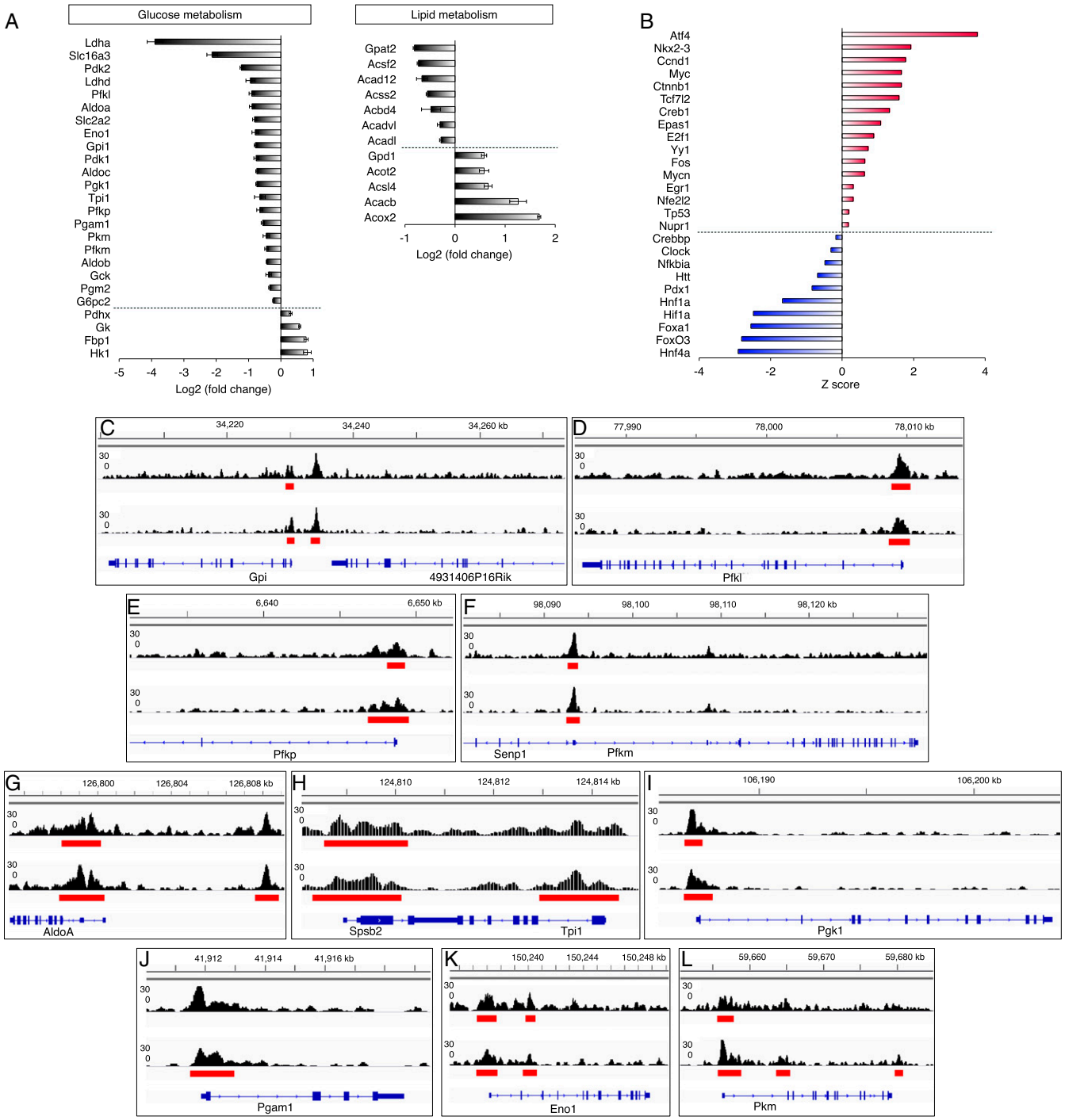

Fig. 6. C2cd4a regulates glycolytic enzymes and "disallowed" genes. (*A*) Log fold-change in expression of selected glycolytic, lipolytic, and disallowed genes in C2cd4a-overexpressing MIN6 cells (RNA sequencing, $n = 3$ each). Data represent means ± SEM (*B*) In silico analysis of upstream transcription factor regulators of C2cd4a based on RNA sequencing. A positive *z*-score suggests activation, while a negative *z*-score suggests inhibition. (*C–L*) Glycolytic genes possessing FoxO1 binding sites (ChIP-seq $n = 2$) in their promoters: (*C*) glucose-6-phosphate isomerase (Gpi); (*D–F*) phosphofructokinase (Pfk); (*G*) aldolase A (AldoA); (*H*) triosephosphate isomerase (Tpi1); (*I*) phosphoglycerate kinase (Pgk1); (*J*) phosphoglycerate mutase (Pgam1); (*K*) enolase (Eno1); and (*L*) pyruvate kinase (Pkm).

alleles of these SNPs with metabolic parameters, combined with long-range DNA binding interaction data as determined by promoter capture HiC in human islets, and plotted them using a webtool (Capture HiC Plotter, www.chicp.org) (36) (*SI Appendix*, Fig. S6). The A risk allele of SNP rs7172432 (where G is the reference allele) is associated with higher fasting glucose, as well as higher glucose and lower insulin during an oral glucose tolerance test (20). The T risk allele of SNP rs4502156 (where C is the reference allele) is associated with higher proinsulin and fasting glucose levels, and lower 2-h glucose levels and lower insulinogenic index (40). SNP rs7163757 was identified as a functional SNP, based on eQTL and reporter assay (21, 47), DNase hypersensitivity peaks—a marker of open chromatin—and transcription factor ChIP-seq (45). Notably, rs7163757 and rs7172432 are in perfect linkage disequilibrium ($r^2 = 1.0$), and harbor a *cis*-eQTL signal (11). While *Vps13c* appears to have modest if any diabetes-predisposing

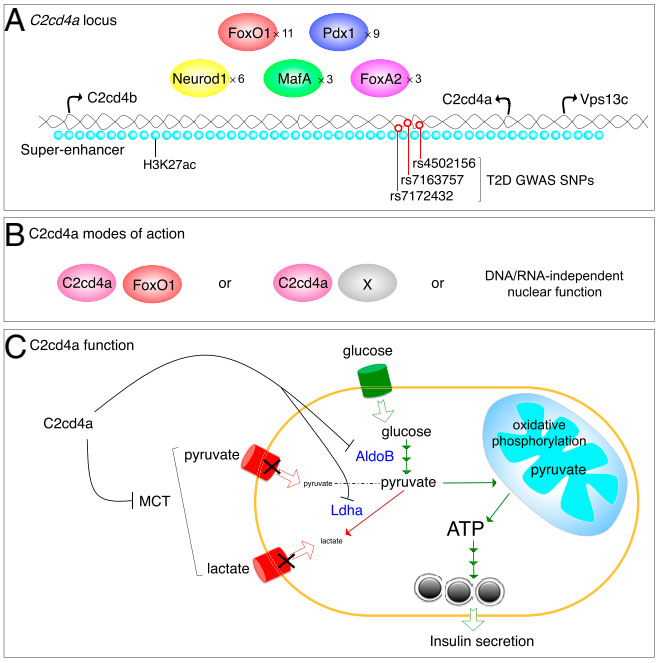

Fig. 7. Proposed model of C2cd4a action in the pancreatic β cell. (*A*) *C2cd4a* resides in a transcription factors-, histone acetylation-, and T2D GWAS SNPs-enriched superenhancer. (*B*) C2cd4a may act as a coregulator for transcription factors, including FoxO1 and others (indicated as X), or exert a DNA/RNA-independent nuclear function. (*C*) C2cd4a represses key β cell disallowed genes, such as lactate dehydrogenase A (Ldha), aldolase B (AldoB), and monocarboxylate transporter (MCT). These disallowed genes are expressed at extremely low amounts to ensure the efficient coupling of glucose metabolism through oxidative phosphorylation to insulin secretion.

effects (21), *C2CD4A* and *C2CD4B* are implicated as putative targets of rs7163757 (47). Furthermore, the present data and indirect evidence in zebrafish (48) strongly support a role of *C2CD4A* in diabetes susceptibility. Human and mouse C2CD4A are highly conserved (58% identity and 64% similarity) and share 2 identical domains that suggest a common function.

Our initial investigations of the effects of C2cd4a gain- and loss-of-function reveal a complex picture. On the one hand, there is a clear impairment of insulin secretion following C2cd4a inactivation. On the other, gain-of-function is associated with a seemingly paradoxical inhibition of the glycolytic cascade. However, we can easily reconcile these findings in the context of the putative role of C2cd4a as a FoxO1 target as well as potential functional partner. Like C2cd4a, FoxO1 is induced under stress, and its loss-of-function is associated with β cell failure, while its gain-of-function is associated with decreased glycolysis and insulin secretion (49). We have termed this regulation "metabolic diapause," a condition in which the FoxO1 transcriptional response seeks to reduce glycolysis in order to prevent generation of toxic intermediates of oxidative phosphorylation that affect β cell survival (44, 50, 51). We propose that C2cd4a is a key partner of FoxO1 in this function, possibly acting as a coregulator at selected genes. Furthermore, C2cd4a appears to suppress disallowed genes, such as *Ldha* (and *Ldhd*), a mainstay of β cell function (42, 43), as well as *AldoB* (along with all members of this gene family), a FoxO1 target activated during starvation or metabolic stress, consistent with *SI Appendix*, Fig. S1 *E* and *F* (51). Furthermore, monocarboxylate transporters are also disallowed in β cells, and 1 member of this class (*Slc16a3*) appears among the C2cd4a targets (Fig. 6*A*). Thus, in addition to repressing the glycolytic cascade, C2cd4a may represent the long-sought repressor of β cell "disallowed" genes (42, 43) (Fig. 7*C*).

We recently demonstrated that induction of Gc (also known as vitamin D binding protein), an α-cell–restricted gene, marks dedifferentiating β cells and contributes to β cell failure (26). Specifically, Gc-deficient β cells failed to induce Aldh1a3, an early marker of β cell dedifferentiation, consistent with a healthier state of β cells (26). While Gc is normally expressed in α-cells, its ablation did not influence glucagon content or glucose-suppressed glucagon secretion (26). Importantly, Gc-deficient mice maintained normal insulin secretion when fed a high-fat diet, and showed an augmented insulin secretory response during hyperglycemic clamps compared to WT (26). Interestingly, C2cd4a gain-of-function in MIN6 cells revealed that it represses Gc expression. This finding suggests that C2cd4a plays a role in cell fate determination, an idea that will be tested in further studies.

This study relies on a technical advance, the development of FoxO1–Venus knockin mice, to overcome 2 limitations to imaging the intracellular dynamics of FoxO1 in β cells, as well as to improving immune detection of the endogenous protein for ChIP-seq experiments, as demonstrated by a 20-fold increase over the number of binding sites detected using a FoxO1 antibody in a previous work (52). Our FoxO1–Venus ChIP-seq most likely modeled the deacetylated, dephosphorylated form of FoxO1 that is active in the nucleus (53). Virtually every gene-encoding component of the insulin/IGF signaling pathway displays a FoxO1 signature, including *FoxO1* itself. Interestingly, unlike *Pdx1*, *MafA*, or *NeuroD1*, whose promoters contain binding sites from multiple transcription factors, thus providing redundancy to the system, only FoxO1 can bind to its own promoter, indicating that this mechanism is nonredundant. This homeostatic loop provides an explanation for the critical role of the loss of FoxO1 expression during diabetes progression, as well as for the associated impairment of Akt signaling that leads to deterioration of β cell function (54, 55).

Another striking FoxO1 target network includes RICTOR and protein translation/processing, indicating a role of FoxO1 function on the balance between protein synthesis, folding, and degradation. In addition to RICTOR itself, many eIFs possess FoxO1 sites, as do critical prohormone processing enzymes such as *Cpe*, *Pam*, and *Pcsk2*, *-4*, and *-6*. Two critical targets in this signaling pathway are *Ppp1r15a*, encoding a regulatory subunit of the type 1 serine/threonine protein phosphatase that dephosphorylates eIF2α (56), and whose down-regulation can contribute to protein misfolding, as well as the endoplasmic reticulum-associated degradation protein, Sdf2l1. The latter's expression increases in FoxO1 knockout β cells, suggesting that FoxO1 inhibits its expression. Sdf2l1 interacts with misfolded proinsulin, delaying its folding (57), and potentially explaining the hyperproinsulinemia of FoxO knockout mice (14).

In conclusion, through a genome-wide analysis of FoxO1 targets in the β cell, we identify *C2CD4A* as a gene that confers human diabetes susceptibility. In addition to providing evidence of an overall role of FoxO1 in the transcriptional network underlying β cell function, the data highlight a heretofore unknown genetic predisposing factor in β cell failure.

Materials and Methods

Animals Care and Diets. Heterozygous leptin receptor-deficient *db/db* mice were purchased from The Jackson Laboratories. Rat insulin promoter (RIP)-driven *Cre* recombinase (RIP-*Cre*) transgenic mice (58) and *Gt(Rosa)26Sor*$^{tm9(Cag\text{-}tdTomato)Hze}$ mice (The Jackson Laboratories) were crossed to heterozygous *db/db* mice to lineage-trace β cells using FACS, with details in *SI Appendix, SI Materials and Methods*. All mice were fed chow diet, unless otherwise specified, and maintained on a 12-h light cycle (lights on at 7:00 AM). Experiments were performed in both male and female mice, as indicated in the figure legends. For calorie-restriction, Venus mice were provided with 70% of normal chow for 4 wk. To induce insulin resistance, Venus mice were fed 60% high-fat diet (Open Source Diet, D12492) for 12 wk. The Columbia University Institutional Animal Care and Utilization Committee approved all experiments.

Generation of Venus Knockin Mice. We purchased BAC clone *RP23-183H8*, which harbors the entire FoxO1 gene, from the BACPAC Resources Center (Children's Hospital Oakland Research Institute). To express GFP (Venus), we obtained the *pCAG:myr-Venus* plasmid from Addgene (#32602). A 15-amino acid linker sequence was placed between the C terminus of FoxO1 and N terminus of Venus to alleviate steric hindrance. We used BAC recombineering to generate FoxO1-Venus ES cells. The detailed protocol and primer sequences are presented in *SI Appendix, SI Materials and Methods*.

Generation of C2cd4a Flox/Flox Mouse. *C2cd4a* consists of 2 exons, the second of which contains the coding sequence. We inserted a loxP site in the first intron, and a second 200-bp downstream of the polyA tail, so that the function of the polyA signal was not affected. We then crossed *C2cd4a* floxed mice with RIP-driven Cre recombinase (RIP-*Cre*) transgenic mice (58) to produce β cell–specific *C2cd4a* knockout mice.

Metabolic Parameters. We performed intraperitoneal glucose tolerance tests (2 g/kg) after a 16-h fast (59). The procedure for hyperglycemic clamps is described in *SI Appendix, SI Materials and Methods*.

FoxO1 ChIP-Seq. The descriptions for islet and ChIP preparation are presented in *SI Appendix, SI Materials and Methods* (26, 60), with ChIP-qPCR primer sequences listed in Dataset S13. Anti-GFP antibody (Abcam, ab290, lot no. GR278480-1) was used for ChIP, and 25 μg chromatin was used per FoxO1 ChIP-seq ($n = 2$). The bandwidth was 200 bp, and the P value cutoff was 1×10^{-7}. All peaks were used for HOMER motif analysis to reveal the consensus FoxO1 sequence (P value of 10^{-292}) (*SI Appendix*, Fig. S7). Thereafter, the top 1,000 60-bp peak sequences (based on peak value) were run through HOMER and MEME with standard settings (–maxsize 60000 –mod zoops –nmotifs 3 –minw 8 –maxw 20 –minsites 100 –maxsites 300 –revcomp) to obtain the probability matrix of the consensus motif (P value of 10^{-38}) (*SI Appendix*, Fig. S8). This FoxO1 consensus motif was used as input for FIMO to scan for occurrences (23). Raw and processed sequencing data were deposited into the MINSEQE-compliant National Center for Biotechnology Information Gene Expression Omnibus database (GSE131947).

H3K27ac ChIP-Seq and Enhancer Motif Analysis. Pancreatic β cells were genetically labeled with *ROSA26-Tomato* fluorescence with *Rip-Cre* allele, and FAC-sorted β cells (~200,000 cells) were used for histone H3K27ac ChIP-seq with anti-H3K27ac antibody (Active Motif, 39133). ChIP was performed as previously described (26, 60), with modifications presented in *SI Appendix, SI Materials and Methods*. H3K27ac peak locations were determined using the MACS algorithm (v1.4.2) with a cutoff of $P < 1 \times 10^{-7}$ (61). Raw and processed sequencing data were deposited in the National Center for Biotechnology Information Gene Expression Omnibus database (GSE131947). ROSE was used to identify enhancers (62) and superenhancers (63). Enhancer motif analysis is described in *SI Appendix, SI Materials and Methods*.

Superenhancer Analysis. MACS peaks identified by H3K27ac ChIP-seq were used as "constituent enhancers" input in ROSE (63). Default settings for stitching distance (12.5 kb) and transcription start site exclusion zone (0 bp–no promoter exclusion) were used. Description for the conversion of human active enhancers to mouse genome is presented in *SI Appendix, SI Materials and Methods*.

CRISPR Mutagenesis of C2cd4a. Guided RNA with a sequence of GGC TCT TGC GGG ACC GAG AT targeting C2cd4a was cloned into pCRISPR-CG01 (GeneCopoeia) with CMV-driven Cas9, as well as selection factors mCherry and neomycin. The protocol is described in *SI Appendix, SI Materials and Methods*.

Live Cell Imaging. Islet preparation for imaging is described in *SI Appendix, SI Materials and Methods*. We used Leica TCS SP8, a confocal laser scanning microscope, for live imaging of Venus islets, and recorded the nuclear translocation of FoxO1–Venus protein, with the following settings: 7-min time interval with 6 time points (a total of 35 min), 488-nm laser with 15% power, HyD (498 to 554 nm) detector, 8,000-Hz scanning speed, 40× objective, 1.1 numerical aperture, 81-μm pinhole, and 64 line average.

Expression of C2cd4a-GFP Fusion Protein Using Adenovirus. The detailed protocol for adenovirus generation and expression is presented in *SI Appendix, SI Materials and Methods*.

RNA Isolation, Quantitative PCR, and RNA Sequencing. We isolated total RNA Nucleospin RNA kit (Macherey–Nagel), and followed previously described protocol for reverse transcription (64). The detailed protocol and primer sequences are presented in *SI Appendix, SI Materials and Methods*. For RNA sequencing, raw and processed data were deposited into the MINSEQE-compliant National Center for Biotechnology Information Gene Expression Omnibus database (GSE132200).

Western Blotting and Imaging. We perform immunoblotting as previously described (65), with modifications and antibody information presented in *SI Appendix, SI Materials and Methods*.

Statistical Analysis. Two-tailed Student's t test and ANOVA were performed with Prism (GraphPad) for quantitative PCR experiments, glucose tolerance tests, and secretogogue-stimulated insulin secretion.

ACKNOWLEDGMENTS. We thank members of the D.A. laboratory for discussions; Thomas Kolar, Ana Flete-Castro, Qiong Xu, Jun Feranil, and Lumei Xu (Columbia University) for technical support; and Irene Miguel-Escalada and Jorge Ferrer (Imperial College London) for the human islet data. This work was supported by NIH Grants T32DK07328 (to T.K.), K01DK114372 (to T.K.), DK64819 (to D.A.), and DK63608 (Columbia University Diabetes Research Center); and by the JPB Foundation (M.A.L. and D.A.).

1. American Diabetes Association, Economic costs of diabetes in the U.S. In 2017. *Diabetes Care* **41**, 917–928 (2018).
2. E. Ferrannini, The stunned beta cell: A brief history. *Cell Metab.* **11**, 349–352 (2010).
3. M. van de Bunt *et al*., Transcript expression data from human islets links regulatory signals from genome-wide association studies for type 2 diabetes and glycemic traits to their downstream effectors. *PLoS Genet.* **11**, e1005694 (2015).
4. A. Mahajan *et al*.; DIAbetes Genetics Replication And Meta-analysis (DIAGRAM) Consortium; Asian Genetic Epidemiology Network Type 2 Diabetes (AGEN-T2D) Consortium; South Asian Type 2 Diabetes (SAT2D) Consortium; Mexican American Type 2 Diabetes (MAT2D) Consortium; Type 2 Diabetes Genetic Exploration by Nex-generation sequencing in muylti-Ethnic Samples (T2D-GENES) Consortium, Genome-wide trans-ancestry meta-analysis provides insight into the genetic architecture of type 2 diabetes susceptibility. *Nat. Genet.* **46**, 234–244 (2014).
5. A. P. Morris *et al*.; Wellcome Trust Case Control Consortium; Meta-Analyses of Glucose and Insulin-related traits Consortium (MAGIC) Investigators; Genetic Investigation of ANthropometric Traits (GIANT) Consortium; Asian Genetic Epidemiology Network–Type 2 Diabetes (AGEN-T2D) Consortium; South Asian Type 2 Diabetes (SAT2D) Consortium; DIAbetes Genetics Replication And Meta-analysis (DIAGRAM) Consortium, Large-scale association analysis provides insights into the genetic architecture and pathophysiology of type 2 diabetes. *Nat. Genet.* **44**, 981–990 (2012).
6. J. C. Florez, Mining the genome for therapeutic targets. *Diabetes* **66**, 1770–1778 (2017).
7. P. M. Visscher *et al*., 10 Years of GWAS discovery: Biology, function, and translation. *Am. J. Hum. Genet.* **101**, 5–22 (2017).
8. K. J. Gaulton *et al*.; DIAbetes Genetics Replication And Meta-analysis (DIAGRAM) Consortium, Genetic fine mapping and genomic annotation defines causal mechanisms at type 2 diabetes susceptibility loci. *Nat. Genet.* **47**, 1415–1425 (2015).
9. S. Guo *et al*., Inactivation of specific β cell transcription factors in type 2 diabetes. *J. Clin. Invest.* **123**, 3305–3316 (2013).
10. S. F. Boj, D. Petrov, J. Ferrer, Epistasis of transcriptomes reveals synergism between transcriptional activators Hnf1alpha and Hnf4alpha. *PLoS Genet.* **6**, e1000970 (2010).
11. A. Varshney *et al*.; NISC Comparative Sequencing Program, Genetic regulatory signatures underlying islet gene expression and type 2 diabetes. *Proc. Natl. Acad. Sci. U.S.A.* **114**, 2301–2306 (2017).
12. L. Pasquali *et al*., Pancreatic islet enhancer clusters enriched in type 2 diabetes risk-associated variants. *Nat. Genet.* **46**, 136–143 (2014).
13. S. C. Parker *et al*.; NISC Comparative Sequencing Program; National Institutes of Health Intramural Sequencing Center Comparative Sequencing Program Authors; NISC Comparative Sequencing Program Authors, Chromatin stretch enhancer states drive cell-specific gene regulation and harbor human disease risk variants. *Proc. Natl. Acad. Sci. U.S.A.* **110**, 17921–17926 (2013).
14. S. C. Talchai, D. Accili, Legacy effect of Foxo1 in pancreatic endocrine progenitors on adult β-cell mass and function. *Diabetes* **64**, 2868–2879 (2015).
15. F. Cinti *et al*., Evidence of β-cell dedifferentiation in human type 2 diabetes. *J. Clin. Endocrinol. Metab.* **101**, 1044–1054 (2016).
16. J. Sun *et al*., Beta cell dedifferentiation in T2D patients with adequate glucose control and non-diabetic chronic pancreatitis. *J. Clin. Endocrinol. Metab.* **104**, 83–94 (2018).
17. B. R. Tennant *et al*., Identification and analysis of murine pancreatic islet enhancers. *Diabetologia* **56**, 542–552 (2013).
18. K. Warton, N. C. Foster, W. A. Gold, K. K. Stanley, A novel gene family induced by acute inflammation in endothelial cells. *Gene* **342**, 85–95 (2004).
19. T. Yamauchi *et al*., A genome-wide association study in the Japanese population identifies susceptibility loci for type 2 diabetes at UBE2E2 and C2CD4A-C2CD4B. *Nat. Genet.* **42**, 864–868 (2010).
20. N. Grarup *et al*., The diabetogenic VPS13C/C2CD4A/C2CD4B rs7172432 variant impairs glucose-stimulated insulin response in 5,722 non-diabetic Danish individuals. *Diabetologia* **54**, 789–794 (2011).

21. Z. B. Mehta *et al*., Changes in the expression of the type 2 diabetes-associated gene VPS13C in the β-cell are associated with glucose intolerance in humans and mice. *Am. J. Physiol. Endocrinol. Metab.* **311**, E488–E507 (2016).
22. T. Kitamura *et al*., The forkhead transcription factor Foxo1 links insulin signaling to Pdx1 regulation of pancreatic beta cell growth. *J. Clin. Invest.* **110**, 1839–1847 (2002).
23. C. E. Grant, T. L. Bailey, W. S. Noble, FIMO: Scanning for occurrences of a given motif. *Bioinformatics* **27**, 1017–1018 (2011).
24. Y. I. Kitamura *et al*., FoxO1 protects against pancreatic beta cell failure through NeuroD and MafA induction. *Cell Metab.* **2**, 153–163 (2005).
25. C. Talchai, S. Xuan, H. V. Lin, L. Sussel, D. Accili, Pancreatic β cell dedifferentiation as a mechanism of diabetic β cell failure. *Cell* **150**, 1223–1234 (2012).
26. T. Kuo *et al*., Induction of α cell-restricted Gc in dedifferentiating β cells contributes to stress-induced β-cell dysfunction. *JCI Insight* **5**, 128351 (2019).
27. M. P. Keller *et al*., The transcription factor Nfatc2 regulates β-Cell proliferation and genes associated with type 2 diabetes in mouse and human islets. *PLoS Genet.* **12**, e1006466 (2016).
28. J. J. Heit *et al*., Calcineurin/NFAT signalling regulates pancreatic beta-cell growth and function. *Nature* **443**, 345–349 (2006).
29. N. Gao *et al*., Foxa1 and Foxa2 maintain the metabolic and secretory features of the mature beta-cell. *Mol. Endocrinol.* **24**, 1594–1604 (2010).
30. X. Feng *et al*., The telomere-associated homeobox-containing protein TAH1/HMBOX1 participates in telomere maintenance in ALT cells. *J. Cell Sci.* **126**, 3982–3989 (2013).
31. M. K. Thomas, N. Rastalsky, J. H. Lee, J. F. Habener, Hedgehog signaling regulation of insulin production by pancreatic beta-cells. *Diabetes* **49**, 2039–2047 (2000).
32. L. Landsman, A. Parent, M. Hebrok, Elevated Hedgehog/Gli signaling causes beta-cell dedifferentiation in mice. *Proc. Natl. Acad. Sci. U.S.A.* **108**, 17010–17015 (2011).
33. M. Kobayashi *et al*., FoxO1 as a double-edged sword in the pancreas: Analysis of pancreas- and β-cell-specific FoxO1 knockout mice. *Am. J. Physiol. Endocrinol. Metab.* **302**, E603–E613 (2012).
34. B. G. Hoffman *et al*., Locus co-occupancy, nucleosome positioning, and H3K4me1 regulate the functionality of FOXA2-, HNF4A-, and PDX1-bound loci in islets and liver. *Genome Res.* **20**, 1037–1051 (2010).
35. A. S. Hinrichs *et al*., The UCSC genome browser database: Update 2006. *Nucleic Acids Res.* **34**, D590–D598 (2006).
36. I. Miguel-Escalada *et al*., Human pancreatic islet three-dimensional chromatin architecture provides insights into the genetics of type 2 diabetes. *Nat. Genet.* **51**, 1137–1148 (2019).
37. R. A. Scott *et al*.; DIAbetes Genetics Replication And Meta-analysis (DIAGRAM) Consortium, An expanded genome-wide association study of type 2 diabetes in Europeans. *Diabetes* **66**, 2888–2902 (2017).
38. E. De Franco *et al*., Dominant ER stress-inducing *WFS1* mutations underlie a genetic syndrome of neonatal/infancy-onset diabetes, congenital sensorineural deafness, and congenital cataracts. *Diabetes* **66**, 2044–2053 (2017).
39. B. Cui *et al*., A genome-wide association study confirms previously reported loci for type 2 diabetes in Han Chinese. *PLoS One* **6**, e22353 (2011).
40. R. J. Strawbridge *et al*.; DIAGRAM Consortium; GIANT Consortium; MuTHER Consortium; CARDIoGRAM Consortium; C4D Consortium, Genome-wide association identifies nine common variants associated with fasting proinsulin levels and provides new insights into the pathophysiology of type 2 diabetes. *Diabetes* **60**, 2624–2634 (2011).
41. D. L. Eizirik *et al*., The human pancreatic islet transcriptome: Expression of candidate genes for type 1 diabetes and the impact of pro-inflammatory cytokines. *PLoS Genet.* **8**, e1002552 (2012).
42. T. J. Pullen *et al*., Identification of genes selectively disallowed in the pancreatic islet. *Islets* **2**, 89–95 (2010).
43. L. Thorrez *et al*., Tissue-specific disallowance of housekeeping genes: The other face of cell differentiation. *Genome Res.* **21**, 95–105 (2011).
44. J. Buteau, A. Shlien, S. Foisy, D. Accili, Metabolic diapause in pancreatic beta-cells expressing a gain-of-function mutant of the forkhead protein Foxo1. *J. Biol. Chem.* **282**, 287–293 (2007).
45. M. A. Schaub, A. P. Boyle, A. Kundaje, S. Batzoglou, M. Snyder, Linking disease associations with regulatory information in the human genome. *Genome Res.* **22**, 1748–1759 (2012).
46. J. Dupuis *et al*.; DIAGRAM Consortium; GIANT Consortium; Global BPgen Consortium; Anders Hamsten on behalf of Procardis Consortium; MAGIC investigators, New genetic loci implicated in fasting glucose homeostasis and their impact on type 2 diabetes risk. *Nat. Genet.* **42**, 105–116 (2010).
47. I. Kycia *et al*., A common type 2 diabetes risk variant potentiates activity of an evolutionarily conserved islet stretch enhancer and increases C2CD4A and C2CD4B expression. *Am. J. Hum. Genet.* **102**, 620–635 (2018).
48. E. A. O'Hare, L. M. Yerges-Armstrong, J. A. Perry, A. R. Shuldiner, N. A. Zaghloul, Assignment of functional relevance to genes at type 2 diabetes-associated loci through investigation of β-cell mass deficits. *Mol. Endocrinol.* **30**, 429–445 (2016).
49. D. Accili, Insulin action research and the future of diabetes treatment: The 2017 banting medal for scientific achievement lecture. *Diabetes* **67**, 1701–1709 (2018).
50. J. Y. Kim-Muller *et al*., Metabolic inflexibility impairs insulin secretion and results in MODY-like diabetes in triple FoxO-deficient mice. *Cell Metab.* **20**, 593–602 (2014).
51. J. Y. Kim-Muller *et al*., FoxO1 deacetylation decreases fatty acid oxidation in β-cells and sustains insulin secretion in diabetes. *J. Biol. Chem.* **291**, 10162–10172 (2016).
52. D. J. Shin *et al*., Genome-wide analysis of FoxO1 binding in hepatic chromatin: Potential involvement of FoxO1 in linking retinoid signaling to hepatic gluconeogenesis. *Nucleic Acids Res.* **40**, 11499–11509 (2012).
53. A. S. Banks *et al*., Dissociation of the glucose and lipid regulatory functions of FoxO1 by targeted knockin of acetylation-defective alleles in mice. *Cell Metab.* **14**, 587–597 (2011).
54. T. Mezza *et al*., Nuclear export of FoxO1 is associated with ERK signaling in β-cells lacking insulin receptors. *J. Biol. Chem.* **291**, 21485–21495 (2016).
55. C. E. Gleason *et al*., Role of insulin-like growth factor-binding protein 5 (IGFBP5) in organismal and pancreatic beta-cell growth. *Mol. Endocrinol.* **24**, 178–192 (2010).
56. T. D. Baird, R. C. Wek, Eukaryotic initiation factor 2 phosphorylation and translational control in metabolism. *Adv. Nutr.* **3**, 307–321 (2012).
57. A. Tiwari *et al*., SDF2L1 interacts with the ER-associated degradation machinery and retards the degradation of mutant proinsulin in pancreatic β-cells. *J. Cell Sci.* **126**, 1962–1968 (2013).
58. P. L. Herrera, Adult insulin- and glucagon-producing cells differentiate from two independent cell lineages. *Development* **127**, 2317–2322 (2000).
59. T. Kuo, J. Y. Kim-Muller, T. E. McGraw, D. Accili, Altered plasma profile of antioxidant proteins as an early correlate of pancreatic β cell dysfunction. *J. Biol. Chem.* **291**, 9648–9656 (2016).
60. T. Kuo *et al*., Genome-wide analysis of glucocorticoid receptor-binding sites in myotubes identifies gene networks modulating insulin signaling. *Proc. Natl. Acad. Sci. U.S.A.* **109**, 11160–11165 (2012).
61. Y. Zhang *et al*., Model-based analysis of ChIP-Seq (MACS). *Genome Biol.* **9**, R137 (2008).
62. W. A. Whyte *et al*., Master transcription factors and mediator establish super-enhancers at key cell identity genes. *Cell* **153**, 307–319 (2013).
63. M. P. Creyghton *et al*., Histone H3K27ac separates active from poised enhancers and predicts developmental state. *Proc. Natl. Acad. Sci. U.S.A.* **107**, 21931–21936 (2010).
64. T. Kuo *et al*., Repression of glucocorticoid-stimulated angiopoietin-like 4 gene transcription by insulin. *J. Lipid Res.* **55**, 919–928 (2014).
65. T. Kuo *et al*., Transcriptional regulation of FoxO3 gene by glucocorticoids in murine myotubes. *Am. J. Physiol. Endocrinol. Metab.* **310**, E572–E585 (2016).